Journal of Luminescence 167 (2015) 167–171

Contents lists available at ScienceDirect

Journal of Luminescence

journal homepage: www.elsevier.com/locate/jlumin

On the quenching of trivalent terbium luminescence by ligand low lying triplet state energy and the role of the $^7F_5$ level: The $[Tb(tta)_3(H_2O)_2]$ case

A.S. Souza [a,*], L.A. Nunes [b], M.C.F.C. Felinto [c], H.F. Brito [d], O.L. Malta [a]

[a] Departamento de Química Fundamental, Universidade Federal de Pernambuco, 50670-901 Recife, PE, Brazil
[b] Instituto de Física de São Carlos, Universidade de São Paulo, 13560-970 São Carlos, SP, Brazil
[c] Instituto de Pesquisas Energéticas e Nucleares-IPEN, 05505-800 São Paulo, SP, Brazil
[d] Instituto de Química, Universidade de São Paulo, 05508-900 São Paulo, SP, Brazil

ARTICLE INFO

Article history:
Received 21 October 2014
Received in revised form
6 May 2015
Accepted 9 June 2015
Available online 25 June 2015

Keywords:
Tb^{3+} Luminescence
Lanthanide coordination compounds
Energy transfer

ABSTRACT

In this work we discuss the observed Tb^{3+} ion luminescence quenching, due to the relative ligand low lying triplet state energy, in the $[Tb(tta)_3(H_2O)_2]$ compound at low and room temperature (tta=thenoyltrifluoroacetonate). Theoretical energy transfer rates, for both multipolar and exchange mechanisms, were calculated and discussed on the basis of selection rules and energy mismatch conditions from the $[Tb(tta)_3(H_2O)_2]$ emission spectra. We have concluded that the exchange mechanism by far dominates, in the present case, and that the long first excited state $^7F_5$ lifetime (in the millisecond scale) plays a crucial role in the Tb^{3+} luminescence quenching.

1. Introduction

One of the most relevant subjects in the study of luminescent lanthanide coordination compounds is the description of the energy transfer processes between the organic ligands and the trivalent lanthanide ion (Ln^{3+}) [1-3]. It is known that energy transfer (forward or back transfer) induces luminescence enhancement or luminescence quenching in Ln^{3+} compound, depending on the relative positions of donor and acceptor energy levels. In the enhancement process the light energy is absorbed by the ligands, in a singlet–singlet transition, and then an intersystem crossing decay populates a lower lying triplet state (T_1) that then transfers energy, non-radiatively, to the Ln^{3+} ion that subsequently emits. This process depends on the resonance condition between the phosphorescence band of the ligand and the ground state absorption spectrum of the Ln^{3+} ion. This does not at all precludes energy transfer (forward and back transfer) straight from the upper excited singlet states to the upper levels of the Ln^{3+} ion.

In the luminescence quenching process the emitting excited state energy of the Ln^{3+} ion is more probable to be transferred to the ligand that then decays to its ground state. This process efficiently occurs when the Ln^{3+} emitting level lies above or close to the T_1 level of the ligand [4,5]. However, before the ligand decays, depending on the energy mismatch situation and temperature, it may retransfer energy to the Ln^{3+} ion, which eventually may be in its first excited electronic state, as in the actual case of the $^7F_5$ level of the Tb^{3+} ion. This level lies at $\sim 2170\ cm^{-1}$ (too high to be thermally populated) above the ground $^7F_6$ level and curiously enough has a long lifetime, as measured in glass and crystalline materials (from 2.8 ms to 22 ms) measured by pumping into the $^7F_2$ level as carried out in Refs. [6,7]. These two facts together with the intramolecular energy transfer selection rules and rates values, for both the multipolar and exchange mechanisms [8], were successfully used in the present work to describe more deeply the Tb^{3+} luminescence quenching observed in the $[Tb(tta)_3(H_2O)_2]$ compound from low up to room temperature.

2. Experimental

2.1. Synthesis

The synthesis of the $[Tb(tta)_3 \cdot (H_2O)_2]$ compound followed a known route for these types of coordination compounds: 30 mL of an aqueous solution of 2.00 g (5.36 mmol) of $TbCl_3 \cdot 6(H_2O)$ and an alcoholic solution of 3.57 g (16.07 mmol) of thenoyltrifluoroacetonate were prepared separately. To the tta ligand solution was added dropwise NaOH (5 mol L^{-1}) until pH ~7. Then,

* Corresponding author. Tel.: +55 7998087125.
E-mail address: adelmosaturnino@hotmail.com (A.S. Souza).

http://dx.doi.org/10.1016/j.jlumin.2015.06.020
0022-2313/

30 mL of an aqueous solution containing terbium chloride was added dropwise to the resulting tta^- solution under stirring at room temperature, adjusting the pH to ~6.5 by addition of a NaOH solution [9]. The reaction mixture was heated at 50 °C to form a white solid. This crystalline compound was filtered, washed with ethanol, dried under reduced pressure at room temperature and stored in a vacuum desiccator.

2.2. Elemental analysis

The quantitative CHN analysis of the $[Tb(tta)_3 \cdot (H_2O)_2]$ complex was performed using a Perkin-Elmer model 2400 microanalyzer. While the contents of the Tb^{3+} ion were determined by complexometric titration with EDTA. The results and the complexometric titration with the disodium ethylenediaminetetraacetic acid (EDTA) salt confirmed the general formula $[Tb(tta)_3 \cdot (H_2O)_2]$: Calc. (%): Tb^{3+}, 18.19; C, 33.47; S, 11.17 and H, 2.22 and found (%): Tb^{3+}, 18.12; C, 32.04; S,10.53 and H, 1.83.

2.3. Luminescence and excitation measurements

The luminescence and excitation spectra were obtained using an spectrofluorometer model SPEX-Fluorolog-2 with double grating 0.22 m monochromators. As the excitation source we use Xe-lamp and a photomultiplier model Hamamatsu/R928 for detection and the slit band pass was 2.5 nm.

2.4. Time-resolved measurements

The time-resolved luminescence measurements were performed by using the third harmonic (355 nm) of a Nd:YAG laser (Surelite I/Continumm, 10 Hz, 5 ns) as excitation source. The transient luminescence signals were dispersed by a monochromator (0.3 m, Thermo Jarrel Ash/82497), equipped with intensified silicon photo-diode array detector model EGG-1456.

The spectra were taken at different temperatures from 10 K to 300 K, by using a Janis Helium Flux Cryostat.

3. Theoretical aspects

The energy transfer between the ligand and the Tb^{3+} ion involves the singlet–triplet (spin-forbidden) and the singlet–singlet (spin-allowed) bands of the ligand and the $a'j' \leftrightarrow \alpha j$ transition lines of the Tb^{3+} ion. This process has been treated in terms of the direct Coulomb and the exchange interactions [8]. For the Coulomb interaction the transfer rate is given by the following equation:

$$W_{Cl} = \sum_{\lambda=2,4,6} \frac{e^2 S_L}{G(2j+1)} \left(\frac{\Omega_\lambda^{ed}}{R_L^6} + \frac{(\lambda+1)\langle r^\lambda\rangle^2 \langle 3\|C^\lambda\|3\rangle^2 (1-\sigma_\lambda)^2}{S_L (R_L^{\lambda+2})^2} \right) |\langle \alpha' j' \| U^\lambda \| \alpha j\rangle|^2 F \quad (1)$$

where j and j' represent the total angular momentum of the Ln^{3+} ion electronic states involved in energy transfer process. S_L is the dipole strength of the ligand transition, G stands for the degeneracy of the donor state and Ω_λ^{ed} are the contributions of the forced electric dipole mechanism to the 4f–4f transition intensity parameters (Judd–Ofelt theory). $\langle r^\lambda\rangle$ are the 4f radial integrals, σ^λ are the shielding factors due to shielding effects produced by the filled 5 s and 5 p sub-shells, R_L is the distance from the Ln^{3+} ion nucleus to the barycenter of the ligand electronic state and F is the donor–acceptor spectral overlap that depends on the appropriate energy mismatch conditions. The exchange intramolecular energy transfer rate (W_{Ex}) is given by the following equation [8]:

$$W_{Ex} = \frac{\langle 4f|L^4\rangle}{(2J+1)} \frac{8\pi e^2}{3\hbar R_L^4} |\langle \alpha' J' \| S \| \alpha J\rangle|^2 \left| \langle \varphi| \sum_i \mu_z(i) s_m(i) |\varphi^*\rangle \right|^2 F \quad (2)$$

$\langle 4f|L\rangle$ is the overlap integral between the 4f orbitals and ligands eigenfunctions, s_m is a spherical component of the spin operator of electron i in the ligand, μ_z is the z-component of its dipole operator and $\boldsymbol{S}$ is the total spin operator of the Ln^{3+} ion. The selections rules on J is obtained using the reduced matrix elements of the unit tensor operators $\boldsymbol{U}^{(\lambda)}$ and those for the total spin operator $\boldsymbol{S}$. From the above matrix elements, as far as J is considered a good quantum number, the selection rules are $|J - J'| = 0$ or 1, for the exchange mechanism, and $J' - J \leq 6 \leq J + J'$ for the Coulomb mechanism, in both cases $J' = J' = 0$ excluded. Although the singlet S_1 has a short lifetime, due to efficient intersystem crossing and internal decays (fluorescence $S_1 \rightarrow S_0$ is rarely observed), energy transfer to the Ln^{3+} ion may occur from S_1 [10].

The spectral overlap factor has been proposed by the following expression [11]:

$$F = \frac{1}{\hbar\gamma} \sqrt{\frac{\ln(2)}{\pi}} exp\left[-\left(\frac{\Delta}{\hbar\gamma} \right)^2 \ln(2) \right] \quad (3)$$

where $\hbar\gamma$ is the (barycenter) band width at half-height of the $T_1 \rightarrow S_0$ transition and Δ is the difference between this transition energy and the energy barycenter of the $\alpha' J' \leftrightarrow \alpha J$ transition. Thus, in resonant, or quasi-resonant conditions, the energy transfer rates are only slightly dependent on the temperature ($\Delta \cong 0$). For back transfer, the rates should be multiplied by the activation energy barrier Boltzmann factor $\exp(-\Delta/k_B T)$ [12].

4. Results and discussion

The emission spectra of the $[Tb(tta)_3\ (H_2O)_2]$ compound measured at low temperature (10 K), under excitations at 398 and 488 nm, in the spectral region characteristic of the Tb^{3+} luminescence, are shown in Fig. 1. The emission under excitation at 398 nm consists only of the tta ligand phosphorescence. In our assumption the tta ligand is excited to the singlet state (S_1) that then decays to the T_1 level from intersystem crossing and then may eventually emit a broad band in the visible (green). The peak (we take as the barycenter) energy position of the phosphorescence maximum intensity is at 540 nm and is in agreement with published data for the $[Gd(tta)_3\ (H_2O)_2]$ compound [9]. Since energy transfer from the S_1 to the $^5D_3$ level (~26300 cm^{-1} from the ground state [13]) is negligible, because the excitation at 398 nm is 1190 cm^{-1} below the $^5D_3$ level, absence of the Tb^{3+}

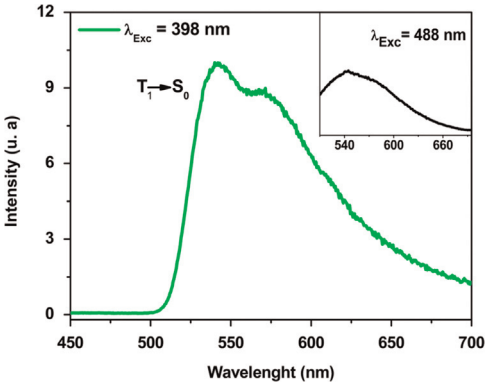

Fig. 1. Emission spectrum of the $[Tb(tta)_3\ (H_2O)_2]$ compound recorded at 10 K under 398 nm excitation. The inset presents emission under 488 nm excitation in resonance with the weak $^7F_6 \rightarrow {}^5D_4$ absorption.

emission is in good agreement with our assumption that the energy transfer from T_1 to the $^5D_4$ level is less efficient when the Tb^{3+} ion is in its ground state. The inset in Fig. 1 shows the Tb^{3+} emission spectrum by direct excitation of the $^5D_4$ level from the ground $^7F_6$ level (488 nm excitation). In this spectrum the Tb^{3+} luminescence was not observed because of the weak absorption coefficient of the Tb^{3+} at 488 nm and the efficient energy transfer from the $^5D_4$ level to the T_1 level due, once the $^5D_4$ level is located at energies slightly above T_1.

Although the $^5D_4$ level barycenter is located slightly above the T_1 level, the usual Tb^{3+} emission at 488 ($^5D_4 \rightarrow {}^7F_6$), 542 ($^5D_4 \rightarrow {}^7F_5$), 582 ($^5D_4 \rightarrow {}^7F_4$) and 621 nm ($^5D_4 \rightarrow {}^7F_3$) were observed under excitation at 355 nm and at 10 K (Fig. 2). It is also observed the tta

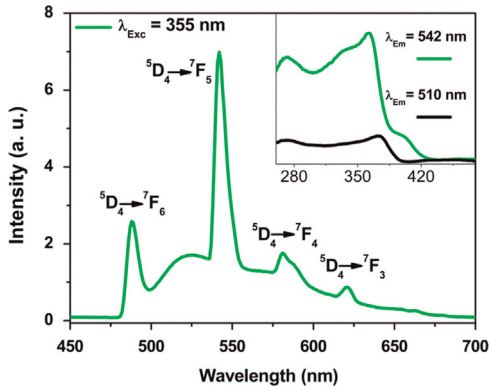

Fig. 2. Emission spectrum of the $[Tb(tta)_3\ (H_2O)_2]$ compound recorded at 10 K under 355 nm excitation. The inset presents excitation spectrum of the complex monitored at emission 542 nm and 510 nm.

phosphorescence. The $^5D_4 \rightarrow {}^7F_5$ transition at 542 nm is in excellent resonance conditions with the T_1 phosphorescence. The excitation spectrum obtained by monitoring the emission in the spectral region of the $^5D_4 \rightarrow {}^7F_5$ transition and in the region 510 nm shows the excitation band of the tta with a maximum at 361 nm (inset in Fig. 2). Although the excitation spectra selective for the Tb^{3+} could, in principal, be obtained monitoring the $^5D_4 \rightarrow {}^7F_{0\text{-}2}$ transitions, they present extremely low intensities, practically preventing their use to distinguish Tb^{3+} and ligand emissions. The absence of the excitation lines $^7F_6 \rightarrow {}^{2S+1}L_J$ of the Tb^{3+} ion clearly indicates the effectiveness of energy transfer from the tta ligand to the Tb^{3+} ion. Since energy transfer from the T_1 level to the $^5D_4$ level is not efficient when the Tb^{3+} ion is in its ground state, the initial energy transfer to the Tb^{3+} ion might occur from the single S_1 to higher energy levels of the Tb^{3+} ion that then decays to the $^5D_4$ level by non-radiative relaxation.

Time-resolved spectroscopy was used to investigate the processes which follow the energy transfer to the Tb^{3+} ion. Although the lifetimes of the $^5D_4$ and T_1 levels in crystals is in the millisecond scale, in the $[Tb(tta)_3\ (H_2O)_2]$ compound they coincide in the range of the microsecond scale. At 10 K and excitation at 355 nm the decay forms of the Tb^{3+} and ligand emissions are exactly equal. This is confirmed by Fig. 3(a). This experimental result indicates that at 10 and 30 K the lifetime and both the energy transfer and back transfer rates between T_1 and $^5D_4$ are very close in value. This process does not primarily involves the ground $^7F_6$ level because the Tb^{3+} ion in the ground $^7F_6$ state is not efficiently depopulated by T_1, as it may checked from the very small values of the reduced matrix elements of the unit tensor operators, $\boldsymbol{U}^{(2)}$, $\boldsymbol{U}^{(4)}$ and $\boldsymbol{U}^{(6)}$, involved in the direct Coulomb interaction energy transfer rates. After the Tb^{3+} ion decays to its lower excited states,

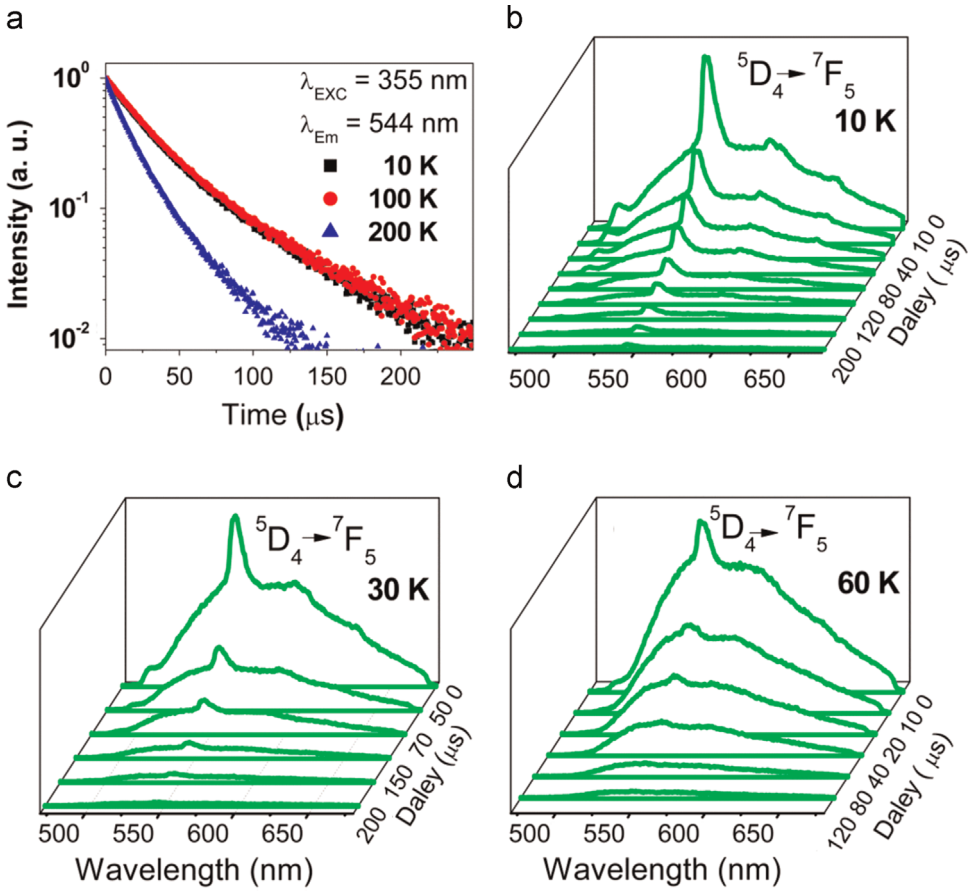

Fig. 3. The transient measurements from the $[Tb(tta)_3\ (H_2O)_2]$ compound obtained at 355 nm (laser excitation). (a) Decay curves monitored at emission 542 nm and (b)–(d) delayed fluorescence taken from 10 K, 30 K and 60 K, respectively.

mainly to the $^7F_5$, which has a long lifetime [6,7], energy transfer to T1 is enormously facilitated also by the exchange mechanism selection rules ($\Delta J=0, \pm 1$) according to Eq. (2). Subsequently, retransfer of energy to the Tb^{3+} ion from T_1, the ion ending back in the $^7F_5$ excited level, is also favored due to the same reasons. Fig. 3 (b) and (c) shows that after 150 μs it is still possible to observe a remaining T_1 phosphorescence in combination with the $^5D_4 \rightarrow {}^7F_J$ transitions.

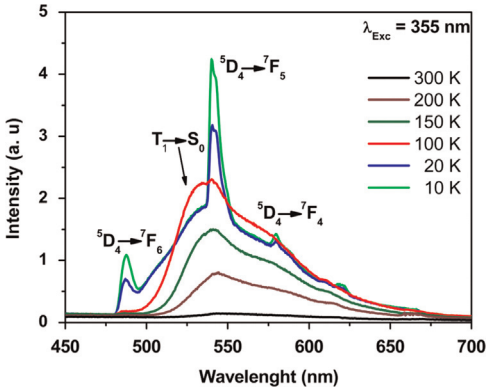

Fig. 4. Emission spectra of the $[Tb(tta)_3\ (H_2O)_2]$ compound recorded at different temperatures under 355 nm excitation.

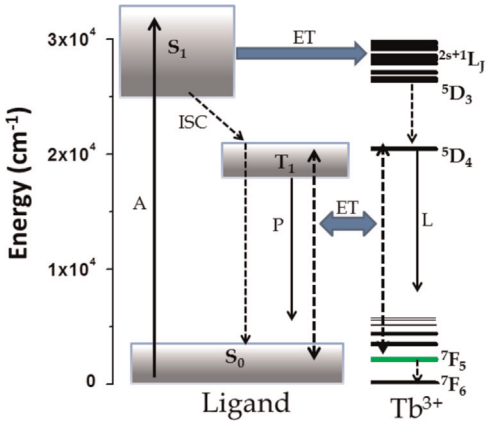

Fig. 5. Energy level diagram and schematic of energy level transfer processes in the $[Tb(tta)_3\ (H_2O)_2]$ compound. Abbreviations: (A) absorption; (P) phosphorescence; (L) lanthanide luminescence; (ISC) intersystem crossing; (ET) energy transfer; (S_1) singlet; (T_1) triplet. Full lines indicative of radiative transitions; dotted lines indicate non-radiative transitions.

Energy transfer from the Tb^{3+} ion to the tta ligand involving the $^7F_4$ level may also contribute to the increase of the population of the $^7F_5$ level due to non-radiative decay $^7F_4 \rightarrow {}^7F_5$. At 60 K, and higher temperatures, the $^5D_4 \rightarrow {}^7F_5$ transition intensity decreases rapidly, practically vanishing within 20 μs, while the T_1 phosphorescence is still observed after a 120 μs delay (Fig. 3(d)). For temperatures higher than 60 K the rate of intersystem crossing from T_1 to S_0 increases rapidly and the overall energy starts being lost mainly through this channel.

Fig. 4 shows the emission spectra obtained in the temperature interval from 10 K to 300 K, under excitation at 355 nm. In the range of 100–300 K the phosphorescence of the tta ligand increases with the decrease of temperature, as expected, and the Tb^{3+} luminescence is totally quenched due the energy transfer from the $^5D_4$ level to T_1. However, at 60 K the tta phosphorescence decreases mainly due to efficient energy retransfer to the $^5D_4$ level, and the $^5D_4 \rightarrow {}^7F_5$ transition is still observed.

Fig. 5 shows the energy level scheme used to represent the level populations. The radiative rate of the $^5D_4$ level ($\sim 10^3\ s^{-1}$) is much less than the energy transfer rate from between the $^5D_4$ and T_1 levels (calculated value. $2.5 \times 10^7\ s^{-1}$ by the exchange mechanism) involving the $^7F_5$ level. To the calculation of the energy transfer rates the wave functions of the $^5D_4$ and ^7F_J states were taken in the intermediate coupling scheme [14]. The theoretical intensity parameters (forced electric dipole mechanism were calculated from the structural data given in Ref. [9] for the case of $[Eu(tta)_3\ (H_2O)_2]$ compound. The numerical estimates for both the multipolar and exchange mechanisms are given in Table 1. The energy transfer rates between the T_1 and $^5D_4$ levels involving the ground $^7F_6$ level (direct Coulomb interaction) is about 10^5 times less than the energy transfer rate involving the $^7F_5$ level (exchange mechanism). It may be argued that the $^7F_5$ abnormally long lifetime is expected to be much shortened in coordination compounds with organic ligands, as compared with the cases of glasses and crystalline systems, and, therefore this could partially affect our conclusions. While appreciating that this lifetime shortening might be operative, we emphasize that even if it drops down to the microsecond scale it would still be much longer than the inverse of the transfer rate by the exchange mechanism. Even though we have not treated in detail the appropriate system of rate equations for level populations according to the energy level diagram shown in Fig. 5, the rather long lifetime of the T_1 phosphorescence (in the microsecond scale)

Table 1
Values of reduced matrix elements and estimates of the transfer rates for the multipolar and exchange mechanisms. Reduced matrix elements were taken from Ref. [13].

	$\lambda = 2$	$\lambda = 4$	$\lambda = 6$
$\lvert\langle[^5D]_4\lVert U^{(\lambda)}\rVert[^7F]_6\rangle\rvert^2$	0.0009	0.0008	0.0013
$\lvert\langle[^5D]_4\lVert U^{(\lambda)}\rVert[^7F]_5\rangle\rvert^2$	0.0142	0.0013	0.0022
$\lvert\langle[^5D]_4\lVert U^{(\lambda)}\rVert[^7F]_4\rangle\rvert^2$	0.0002	0.0022	0.0014
$\langle r^\lambda\rangle(cm^\lambda)$	2.302	1.291	1.501
σ_λ	0.600	0.136	0.001
$\Omega_\lambda^{ed}(cm^2)$	0.020×10^{-20}	0.002×10^{-20}	0.010×10^{-20}
$R_L = 4.50$ Å $S_L = 3.49 \times 10^{-40}$ (e.s.u)^2 cm^2 $\lvert\langle\varphi\rvert\sum_i \mu_z(i)s_m(i)\rvert\varphi^*\rangle\rvert^2 = 10^{-36}$(e.s.u)^{2}cm^2			
$\lvert\langle[^5D]_4\lVert S\rVert[^7F]_6\rangle\rvert^2 = 0.000$ $\lvert\langle[^5D]_4\lVert S\rVert[^7F]_5\rangle\rvert^2 = 0.621$ $\lvert\langle[^5D]_4\lVert S\rVert[^7F]_6\rangle\rvert^2 = 1.139$			
Tb^{3+} transition	Ligand transition	Multipolar mechanism (s^{-1})	Exchanger mechanism (s^{-1})
$^7F_6 \leftrightarrow {}^5D_4$	$S_0 \leftrightarrow T_1$	3.2×10^2	0
$^7F_5 \leftrightarrow {}^5D_4$	$S_0 \leftrightarrow T_1$	1.3×10^3	2.5×10^7

is certainly due to the fast resonant energy exchange between the T_1 and $^5D_4$ levels.

5. Conclusion

We have synthesized and characterized the $[Tb(tta)_3(H_2O)_2]$ compound and have analyzed more deeply, on experimental and theoretical basis, the luminescence quenching of the Tb^{3+} ion in this case, where the tta ligand T_1 peak phosphorescence and terbium $^5D_4 \rightarrow {}^7F_5$ transition (energy barycenters) are practically in resonance. Although there experimental limitations in the excitation spectra selective for the Tb^{3+}, the experimental data suggest the effectiveness of energy transfer from the tta ligand to the Tb^{3+} ion. In our spectral transient measurements, between 10 K and 60 K the Tb^{3+} luminescence is actually observed, however, it disappears above 60 K at a slower rate than does the T_1 phosphorescence. This behavior is in part due to the temperature dependence of the intersystem crossing rate from T_1 to S_0 and the resonance conditions between T_1 and $^5D_4$. We have discussed, both qualitatively and quantitatively, the energy transfer mechanisms involved in the luminescence quenching and the origin of the Tb^{3+} emission observed at low temperatures. Our conclusion is that the luminescence quenching observed in $[Tb(tta)_3(H_2O)_2]$ is mainly the result of a balance between the fast energy exchange between T_1 and the $^5D_4$, mediated by the dominant exchange mechanism involving the first excited Tb^{3+} $^7F_5$ level, and energy loss via the intersystem crossing channel from T_1 to S_0. The fact that the $^7F_5$ level has an long lifetime, at least as observed in glass and crystalline materials, plays a crucial role in this balance.

Acknowledgments

We would like to acknowledge the financial support of the Coordenacão de Aperfeicoamento de Pessoal de Nível Superior (CAPES), and Instituto Nacional de Nanotecnologia para Marcadores Integrados (INAMI).

Reference

[1] K. Binnemans, Chem. Rev. 109 (2009) 4374.
[2] J.C.G. Bünzli, et al., Coord. Chem. Rev. 254 (2010) 2623.
[3] G.F. de Sa, O.L. Malta, C. De Mello Donega, A.M. Simas, R.L. Longo, P.A. Santa-Cruz, E.F. da Silva Jr., Coord. Chem. Rev. 196 (2000) 165.
[4] M. Latva, et al., J. Lumin. 75 (1997) 149.
[5] S. Sato, M. Wada, Bull. Chem. Soc. Jpn. 43 (1970) 1955.
[6] U.N. Roy, et al., Appl. Phys. Lett. 86 (2005) 151911.
[7] K. Rademaker, W.F. Krupke, R.H. Page, S.A. Payne, K. Peterman, G. Huber, A. P. Yelisseyev, L.I. Isaenko, U.N. Roy, A. Burger, K.C. Mandal, K. Nitsch, J. Opt. Soc. Am. B **21** (2004) 2117.
[8] O.L. Malta, J. Non-Cryst. Solids 354 (2008) 4770.
[9] O.O.L. Malta, H.F. Brito, J.,F.,S. Menezes, F.R. Gongalves e Silva, S. Alves Jr., F. S. Farias Jr, A.V.M. de Andrade, J. Lumins 75 (1997) 255.
[10] I.M. Alaoui, J. Phys. Chem. 99 (1995) 13280.
[11] O.L. Malta, J. Lumin. 71 (1997) 229.
[12] W.M. Faustino, L.A. Nunes, I.A. Terra, M.C. Felinto, H.F. Brito, O.L. Malta, J. Lumin. 137 (2013) 269.
[13] W.T. Carnall, H. Crosswhite, H.M. Crosswhite, Energy level Struture and Transition Probabilities of the Trivalent Lanthanides in LaF_3, The Johns Hopkins University, 1977.
[14] G.S. Ofelt, J. Chem. Phys. 38 (1963) 2171.